Chapter 3
Methodology

3.1 General

The success of underground mining, particularly in depillaring panels, largely depends on the stability of the pillars, roof and floor. The stability of the pillars is the prime focus. Understanding the pillars and caving behaviour of overlying strata is important for the assessment of the stability of underground depillaring panels. The objectives of the present study are to develop a time-dependent constitutive model of a coal pillar and an explicit caving simulation approach of a depillaring panel so that the appropriate numerical model can be constructed.

Geotechnical engineering increasingly depends on numerical simulation techniques to manage complex geo-mining conditions. These techniques provide a comprehensive approach to modelling structures, considering various geo-mining complexities. With high computational speed, numerical methods enable the simulation of large structures within a reasonable timeframe. This study employed $FLAC^{3D}$ (Fast Lagrangian Analysis of Continua in three dimensions), a widely used numerical software based on the finite difference method. $FLAC^{3D}$ is renowned for its application in geotechnical analyses of soil, rock, groundwater, constructions, and ground support. It is also used for engineering design, safety prediction, research, testing, and failure back-analysis. This software uses an explicit finite volume formulation to accurately model complex behaviours involving multiple stages, large displacements and strains, non-linear material properties, and unstable conditions, including widespread failure or total collapse. $FLAC^{3D}$ solves ordinary differential equations in a time-stepped simulation of the structure by approximating the differential operator and replacing derivatives with differential quotients.

In this study, an attempt has been made to develop a time-dependent constitutive model and explicit caving simulation approach for an underground depillaring panel. The methodology for studying the time-dependent behaviour of the coal pillar is divided into two stages. In the first stage, a constitutive model was considered and modified to incorporate the phenomenon of reduction of strength parameters with time. In the second stage, a scheme of simulation procedure is developed by incorporating the constitutive model to assess the effect of time on pillar strength is discussed in section 3.2.3. Similarly, for the explicit caving simulation approach, the methodology adopted by using $FLAC^{3D}$ to simulate the caving behaviour is discussed in section 3.3.

3.2 Development of a constitutive model for coal mass

To develop a time-dependent constitutive model, one must know a coal pillar's time-dependent behaviour. From the literature, it was observed that the pillars are designed to be long-term stable, but over time, because of the scaling/side spalling of the pillar's strength reduces and leads to failure of the pillar. The time-dependent failure mechanism and the development of time-dependent constitutive models are explained in detail in the following sub-chapters.

3.2.1 Coal pillar failure mechanism

Pillars can be divided into a maximum of three different zones, namely elastic, plastic and crushing. It is to be noted that corners are more stressed compared to the core of the pillar. As the stress increases, the sides and corners transition from elastic to plastic, eventually reaching the crushing zone. This process occurs based on the strength level of the applied stress, causing the corners and sides to yield first. From the literature (Zhang and Wang 2019; He et al. 2022; Zhang et al. 2022), it was taken as the stress region below the overlying strata's load (tributary area load) is considered a crushing zone. The stress region from the crushing zone to the peak stress point is the plastic zone region, and the remaining stress region is considered the elastic zone region. Developed pillars are designed for long-term stability to protect the surface features. The load on the pillars remains the same, but with time, the strength of the material reduces if it comes under the plastic region. Fig. 3.1 shows a conceptual model of a pillar failure mechanism with respect to the time/age of the pillar. Fig. 3.1a, b and c depict the failure process of a pillar with age. Fig. 3.1a_1, b_1 and c_1 show the corresponding stress distribution profile within the pillar at various stages (ages). Zones I, II and III represent the pillar's crushing (outer), plastic (intermediate) and elastic zones (middle). After the pillars are formed during the development stage, the pillar shows almost the overlying strata's load (tributary area load). With the increasing age of the pillar, cracks developed, and a minor spalling of the pillar took place, as shown in Fig. 3.1a_1. With further increasing the age of the pillar, the outer zones fail (crushing zone), and the load of the failed zones is transferred to adjacent zones (i.e., plastic zone region). As a result of load transferring, the starting point of the elastic zone shows peak stress (Fig. 3.1b_1). The presence of an elastic zone indicates the stability of the coal pillar. On the other side, a large crushing and plastic zone indicates the pillar's instability. With increasing time (i.e., the pillar's age), the crushing zone's area also increases (i.e., gradual spalling of the pillar is observed). As a result, the plastic zone moves towards the elastic zone area, which automatically decreases the elastic zone. The shape of the pillar becomes an hourglass (Fig. 3.1c) due to the side spalling, and eventually, it may fail. Before the pillar's failure, the pillar had only crushing and plastic zones with a peak stress, as shown in Fig. 3.1c$_1$. As a result, the stress profile along the middle section changes from an M-shaped induced stress to inverted V-shaped induced stress, as shown in Fig. 3.1a$_1$, b$_1$, and c$_1$. The failure process of standing/ leftover pillars shows that the mechanism of pillar failure is time-dependent.

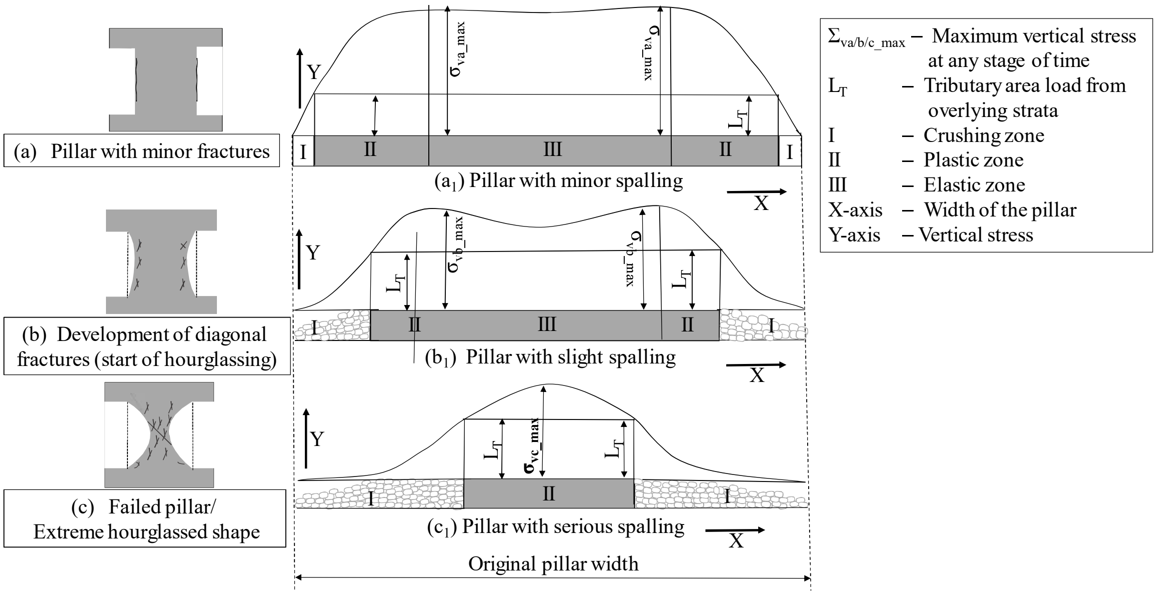

Figure 3.1: A conceptual model of a pillar failure mechanism at constant load with respect to time/age (not on scale)

It is to be noted that the pillars are designed for long-term stability, considering sufficient FOS. Further, it is to be known that the strength decreases with time. So, in the field, various coal pillars also fail in due course of time. Fig. 3.2 shows the complete stress-strain behaviour of a sample replicating a lab-scale coal pillar at different ages with different tributary area loading conditions. Fig. 3.3 illustrates the strain v/s time of a coal pillar at various tributary area load conditions. When a coal pillar is loaded up to its peak strength (point A, as shown in Fig. 3.2), it eventually fails and enters into the residual phase. In Fig. 3.2, curve OAD shows the short-term strength of a coal pillar when it is loaded with a σ_A stress, as shown in Fig. 3.3a. Fig. 3.3a shows the strain v/s time plot when the pillar is loaded with σ_A stress. The average stress at this stage on the pilar is σ_A, and the strain will be ε_A. At this stage, the pillar goes under post-failure behaviour and eventually fails in a shorter span of time. In the strain v/s time graph of Fig. 3.3a, the strain exponentially increases in a shorter span, as denoted by dotted lines. When the applied load (tributary area stress) is less than the peak strength of the pillar, spalling initiates and fails after some time. A coal pillar loaded up to point B (i.e. with the stress of σ_B as shown in Fig. 3.3b) will terminate in a rupture at $B^{|}$ after a longer time ($t_B^{|}$). The corresponding strain value at time t_B is ε_B, and after the time $t_B^{|}$, the axial strain increased to $\varepsilon_B^{|}$ as shown in Fig. 3.2 and Fig. 3.3b. Once the strength reaches $B^{|}$ point, the strength parameters do not allow it to bear the load, so it will go into the residual phase and follow the softening path. Similarly, a coal pillar loaded up to point C (i.e. with the stress of σ_C as shown in Fig. 3c) will terminate in a rupture at $C^{|}$ after a much longer time ($t_C^{|}$) with axial strain values ε_C at time t_C and $\varepsilon_C^{|}$ after a time $t_C^{|}$ as shown in fig. 3.2 and fig. 3.3c. Meanwhile, a pillar loaded at I (damage initiation point) will terminate in rapture at $I^{|}$ after much longer than cases B and C. Below point I, theoretically, there will not be a creep phenomenon happening in the pillar, and this pillar will be very long stable. For cases B and C, after reaching the axial strain of $\varepsilon_B^{|}$ and $\varepsilon_C^{|}$, an exponential uncontrolled increase of axial strain was observed, as denoted in dotted lines (as shown in Fig. 3.3b and c), which indicates the failure of the coal pillar.

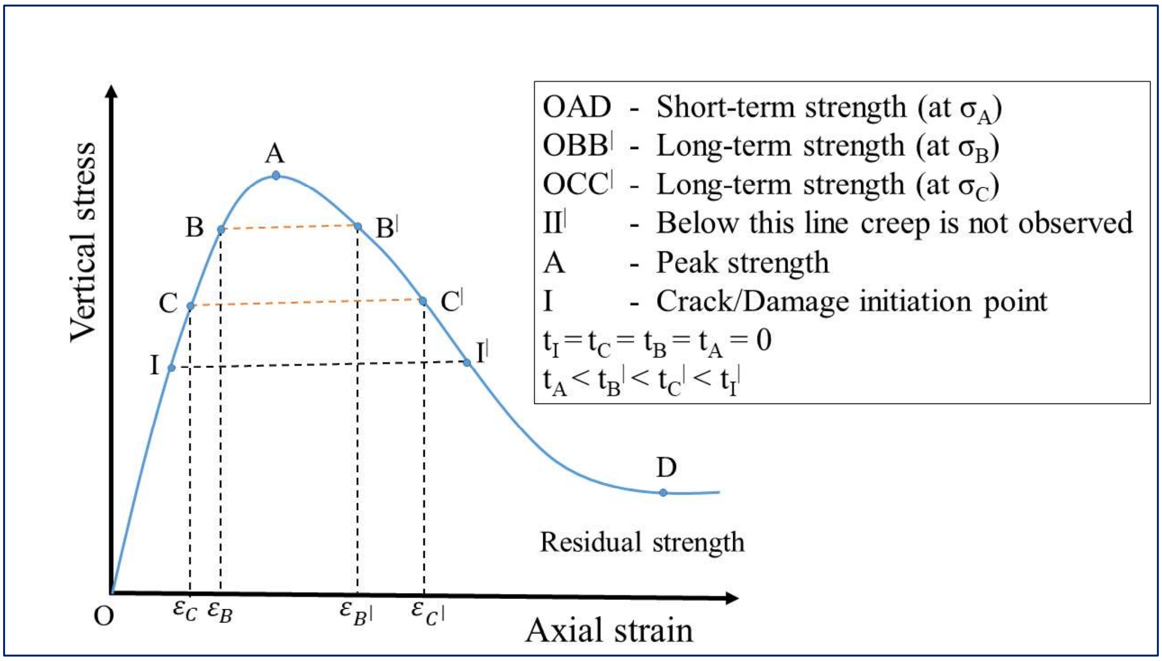

Figure 3.2: The complete stress-strain behaviour of the coal sample

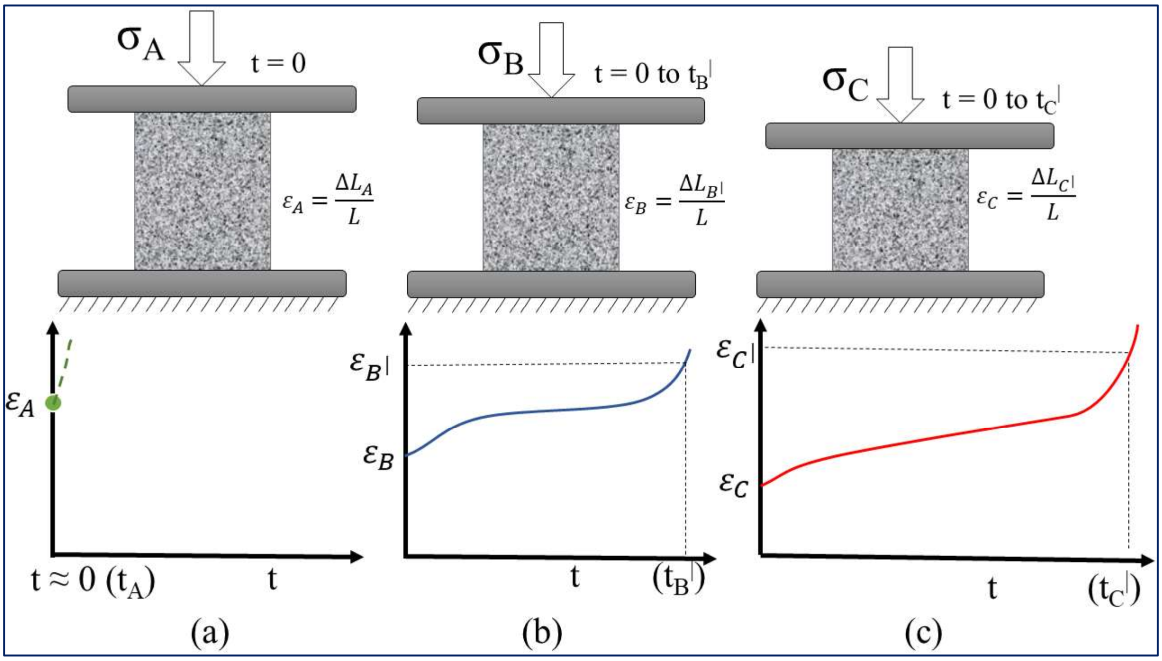

Figure 3.3: Loading of samples at different stress levels ($\sigma_A > \sigma_B > \sigma_c$) and times ($t_A < t_B^{|}$ $< t_C^{|}$)

3.2.2 Time-dependent constitutive model

From the literature it was observed that the strength of the coal pillar decreases with time.

Thus, a time-dependent constitutive model is required to properly understand stress-strain behaviour with time using numerical simulation. In strain-softening constitutive models, generally, strength parameters are reduced with plastic strain. Some researchers (Murali Mohan et al. 2001; Singh et al. 2011b, 2016; Kumar et al. 2023a, b) considered linear decrement of strength with plastic strain, while others researchers (Jaiswal and Shrivastva 2009; Gadepaka et al. 2024) considered exponential decrement. However, it has been observed that the crack/yielding initiation started before reaching its peak/ultimate strength, i.e., crack/yielding initiation strength. Based on this phenomenon, a Hoek-Brown failure constitutive model (Hoek and Brown 1980) was considered and modified to implement the Time-dependent strain-softening behaviour. This Hoek-Brown constitutive model was widely used in pillar design, as expressed in equation 3.1.

$$\sigma_1 = \sigma_3 + \sigma_{ci}\left(m + \frac{\sigma_3}{\sigma_{ci}} + s \right)^a \quad \text{-- (3.1)}$$

Where "*m, s* and *a* are the strength parameters of the rock mass, σ_1 and σ_3 are the maximum and minimum principal stresses, σ_{ci} is the uniaxial compressive strength, and *a* is constant". Fig. 3.4 shows the strain-softening behaviour of rock mass properties with the time-dependent constitutive model. The constitutive model was developed by considering the time-dependent failure of the coal/rock mass when a constant load below the peak strength was applied. The path OIA in Fig. 3.4 shows the instantaneous behaviour of an element. Crack/yield initiation is observed before the peak strength is reached. The rock mass strength parameters (*m* and *s*) at the crack/yield initiation point (at point I in Fig. 3.4) are denoted by m_c and s_c, where '*c*' is the yield strength. After crack initiation, the material will bear some load, develop negligible plastic strain, and fail after a time *t*. After failure, the strength exponentially decreases and enters into the residual phase. To represent this phenomenon, two parameters are needed: ultimate peak strength properties over time and residual strength with plastic strain. If t = 0, then equations 3.2

and 3.3 are used to calculate the peak strength parameters. Whereas for t > 0, the non-linear exponential function (equations 3.4 and 3.5) was considered to calculate the peak strength parameters (m_{pt} and s_{pt}) over time as follows:

if t = 0 then

$$\begin{cases} m_{pt} = m_c & (3.2) \\ s_{pt} = s_c & 3.3) \end{cases}$$

if (t > 0) then

$$\begin{cases} m_{pt} = m_c + \left(m_p - m_c\right) \times e^{(-\beta \times t)} & (3.4) \\ s_{pt} = s_c + \left(s_p - s_c\right) \times e^{(-\beta \times t)} & (3.5) \end{cases}$$

Where " '*t*' is the age of the yielded element in the pillar and '*β*' is the constant that defines the peak reduction parameter". The peak reduction parameter with time accumulates all the external parameters (moisture, humidity, chemical weathering, etc) which influence the rate of strength reduction. During the residual phase, the reduction of strength parameters from peak to residual comes in the softening phase. In this phase, the strength parameters (*m* and *s*) decrease relative to the softening parameter (plastic shear strain). Another exponential function (equations 3.6 and 3.7) is used to estimate the residual strength parameters with respect to both plastic strain and time.

$$m_{rt} = m_r + \left(m_{pt} - m_r\right) \times e^{(\alpha \times \gamma_p)} \quad (3.6)$$

$$s_{rt} = s_r + \left(s_{pt} - s_r\right) \times e^{(\alpha \times \gamma_p)} \quad (3.7)$$

Where "m_{rt} and s_{rt} are the residual strength parameters with respect to time, m_r and s_r are the residual strength parameters, 'α' is the constant that defines the rate of softening, and γ_p is the plastic strain of a particular element".

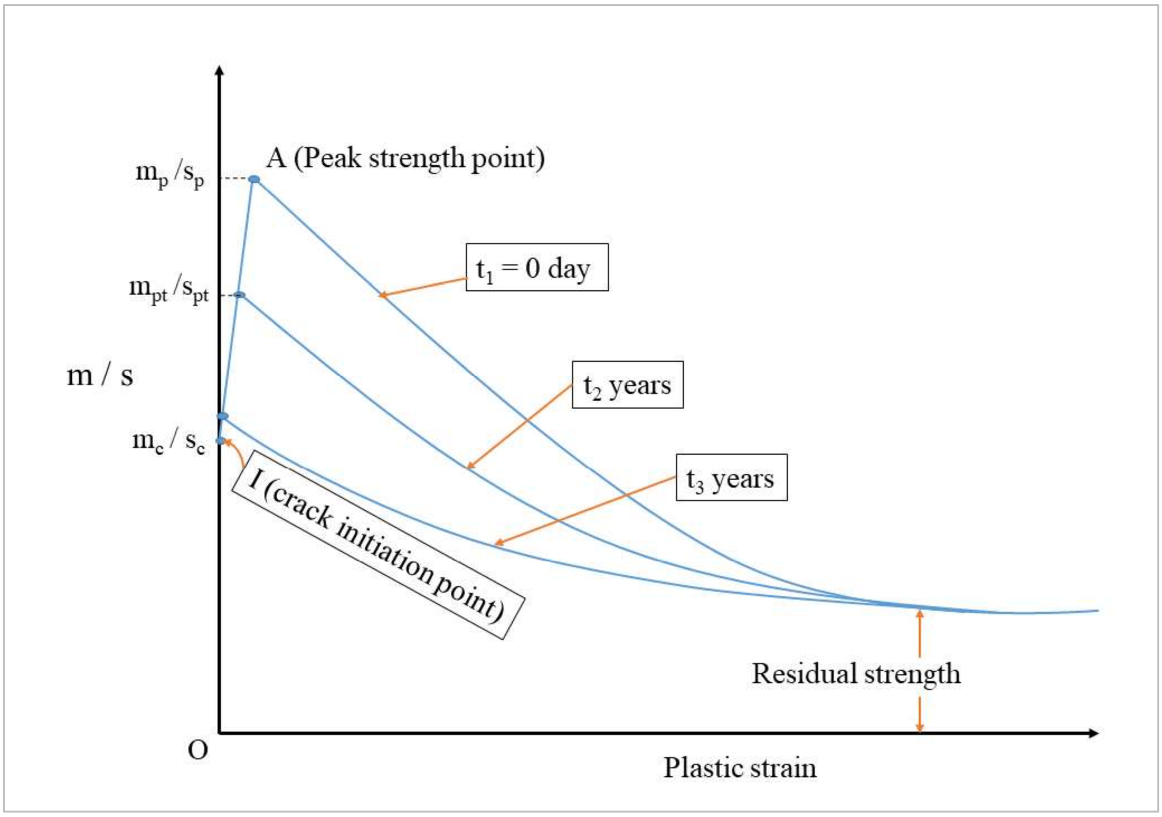

Figure 3.4: Typical behaviour of Hoek-Brown rock mass strength properties with time ($t_1 < t_2 < t_3$)

3.2.3 Generalised simulation procedure

The terminology used in this simulation process is explained in detail to facilitate an easy understanding of the implementation of the constitutive model. After preparation of the model assigning material properties and boundary conditions, the model has been simulated in different stages of age. Here, stage refers to the age of the pillar. After the development of the pillar, all the elements/zones were assigned a zero-yielding age. It is to be noted that the yielding age of the individual zone is different from the age of the pillar. For instance, if none of the elements/zones yielded, the yielding age of the element will be zero as the age of the pillar may be 'A' years (where A may be 1 year). If the model becomes under an un-equilibrium condition at the age of 'A' days, then the life is called 'A'. Different FISH modules are used at various stages of the simulation to accommodate these features in the model. The detailed simulation process is shown in

Fig. 3.5. The process of assigning the yielding age of the elements within the pillar at different stages is shown in Fig. 3.6. The scheme implemented in the model using FISH modules at various simulation stages. FISH has a facility to store additional extra parameters for any elements. Using this capability, the age of the element in days was stored in the zone/element memory, which is used for further calculations. It is explained in the following paragraph.

After the model was developed, material properties and boundary conditions were assigned. The age of the pillar was set to A = 0 days, and every element is assigned zero yielding age i.e. $t_i = 0$ days, where i is the element ID (assigned 1 to N) as shown in Fig. 3.6a. The model was then solved to an equilibrium condition. If the model reaches equilibrium condition, then the life of the pillar is greater than 1 day. If not, the life of the pillar is zero days. Once it reaches the equilibrium condition, a FISH module is used to check and analyse the yielding state of each element within the pillar ($i = 1$ to N). At this stage, if any element undergoes the yielding stage, another fish module, with the help of the extra parameter, assigns the age of the yielded elements as $t_i = 1$ (i.e. $t_i = t_i + 1$) days. The age of non-yielded elements remains at 0 days until they go to a yielding state. At this stage, another fish module is employed to update the material properties to the yielded elements as a function of plastic strain and age (using equations 3.4 and 3.5 for peak and 3.6 and 3.7 for residual phase). The properties of non-yielded elements are updated using equations 3.2 and 3.3. Generally, after the pillar formation on day 1, the corners are yielded, so the age of the corners is changed from 0 days to 1 day, as shown in Fig. 3.6b. If the loop is completed (i.e. all the elements are analysed) at this stage, another FISH function calculates the average axial strain of the pillar and saves it in the data file. After this stage, the model was solved for the next age ($A = A + 1$). In this stage, if any new element (i) comes to a yielding state, the pre-defined FISH module assigns the life of the newly yielded elements as $t_i = 1$ day. The yielding age of the previously yielded elements was increased from 1 day to 2 days, and the non-yielded element age remained at 0 days, as shown in Fig. 3.6c. As discussed in the earlier stage, the material properties of the yielded elements will be updated according to their yielding age by using equations 3.4,3.5,3.6 and 3.7. Similarly, the properties of non-yielded elements are updated using equations 3.4 and 3.5. After all the elements are analysed, the axial strain of the pillar is saved. After that, the simulation is solved for the next day until the model reaches its un-equilibrium condition. The next subsequent stages with the updation of the yielding age of the yielded elements are shown in Fig. 3.6d, e and f. After the complete yielding of all the elements, the pillar fails; at this stage, the life of the pillar (*T*) is 5 days (i.e. stage number), as shown in Fig. 3.6f. After all the elements in the pillar yielded a continuous increasing of axial strain was observed at this stage the model continuously runs without reaching the average stress ratio of approximately 1×10^{-5}. At this stage the model is terminated manually.

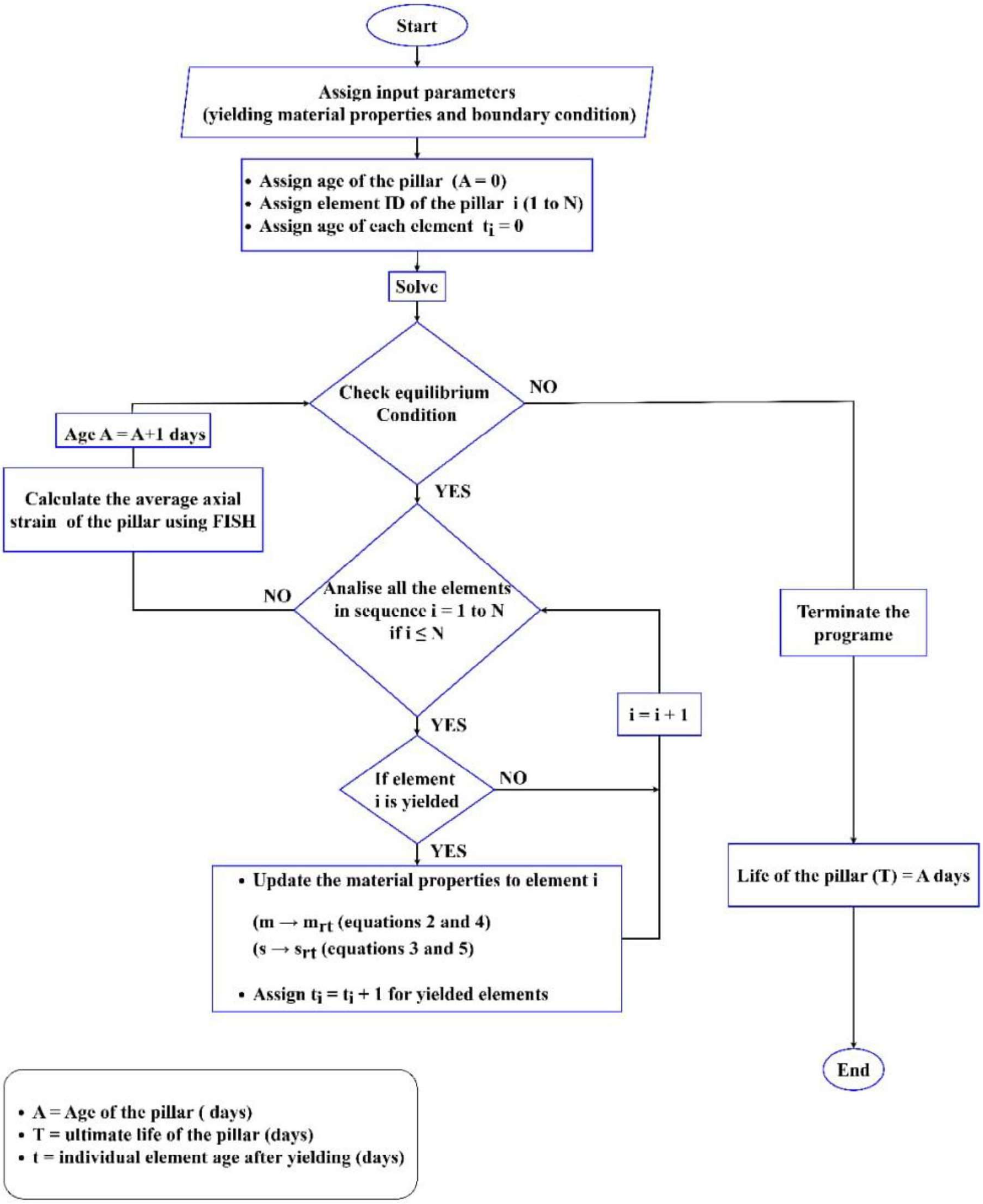

Figure 3.5: Procedure of scheme of simulation

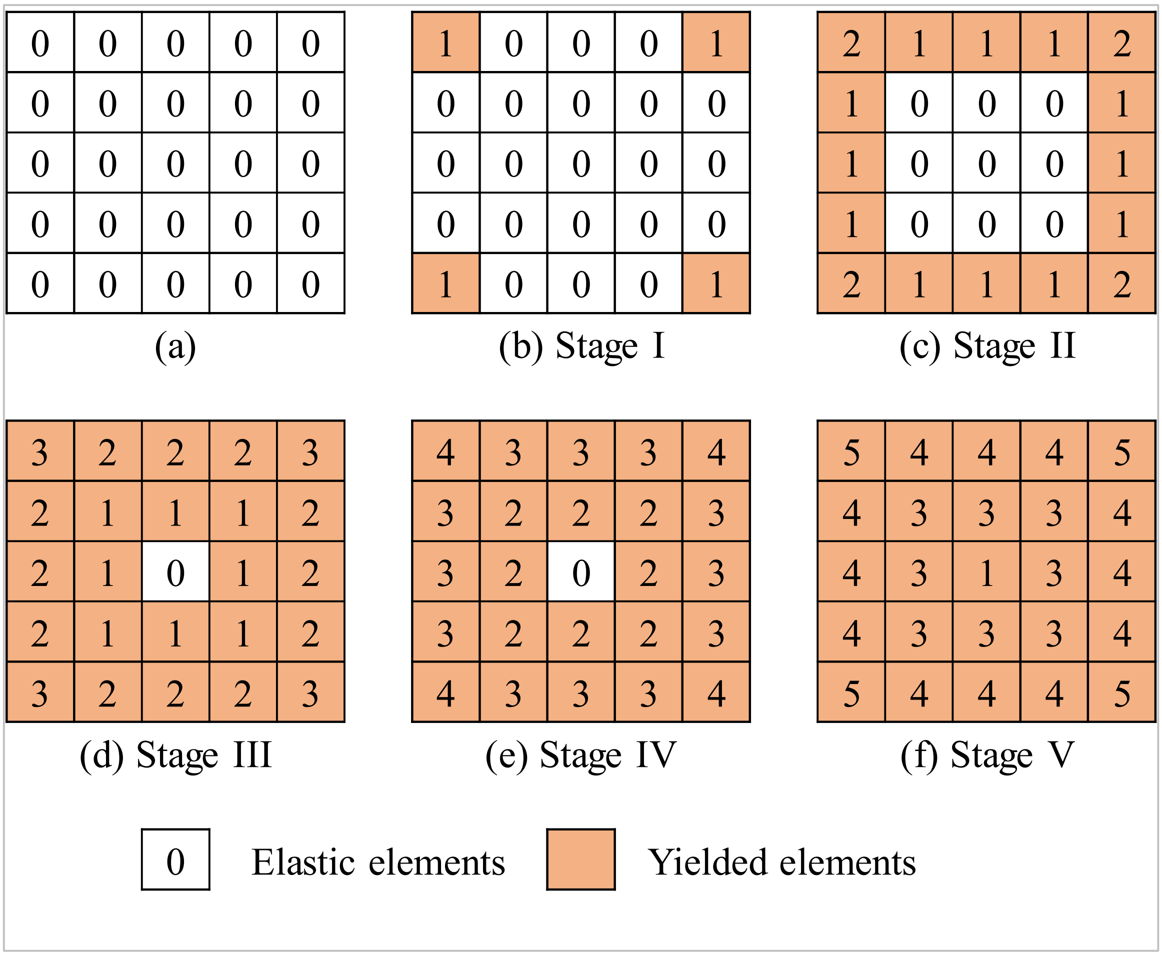

Figure 3.6: A typical yielding process of the elements within the pillar

3.3 Explicit caving simulation approach

During the progressive advancement of goaf, the different layers in the roof are cave and settle on the floor due to the presence of weak bonding or the presence of weak parting planes. The previous approaches described in the literature review are implicit approaches, but with the availability of computational speed and memories, an explicate approach has been proposed using continuum modelling for the simulation of caving behaviour. A three-dimensional finite difference modelling approach FLAC^{3D} (2015) has been used for the implementation of the proposed scheme. The software has an interface facility and solves on large strain mode. Based on the availability of the software package FLAC^{3D}, interface elements have been used as a parting plane for simulation. A linear elastic-perfectly plastic coulomb shear strength criterion has defined the constitutive model of the interface. With the implementation of interface elements, the layers in the roof are liable to separate from one another.

A large strain model is to be simulated in each stage of pillar extraction. The model runs for gaining an equilibrium condition with an average stress ratio of $1e^{-5}$ for each stage. The overhang strata started sagging after getting separated from others due to the yielding of the strata. The displacement of all the grid points of the floor of roof 1 (immediate roof) at every 100 time-steps has to be monitored. Because of the plastic flow nature, these separated layers may be sage with uncontrolled vertical displacements, indicating penetration in the model. In fact, penetration is not possible in the practical sense. Thus, it has to be restricted. $FLAC^{3D}$ has a facility of controlling the internal variables through its in-built functions during the simulation. During this process, a FISH module shall be used to monitor the vertical displacement of the immediate roof (roof 1). If the vertical displacement of a grid is nearly equal to the height of extraction, the FISH module restricts the penetration of the roof into the floor by attaching the grid to the nearest grid point on the floor. The immediate roof layer supports the upper layers and allows them to settle on it. After all the pillars are extracted and the overlying strata settle, the model reaches its equilibrium stage and is terminated. The stopping criteria were adopted as suggested by researchers in the literature, where the model was considered to have converged when the average stress ratio reached approximately 1×10^{-5} . This process reasonably resembles the natural caving behaviour. Understanding of the goaf properties is not required. Fig.3.7 shows the scheme of the simulation flow chart used in this study.

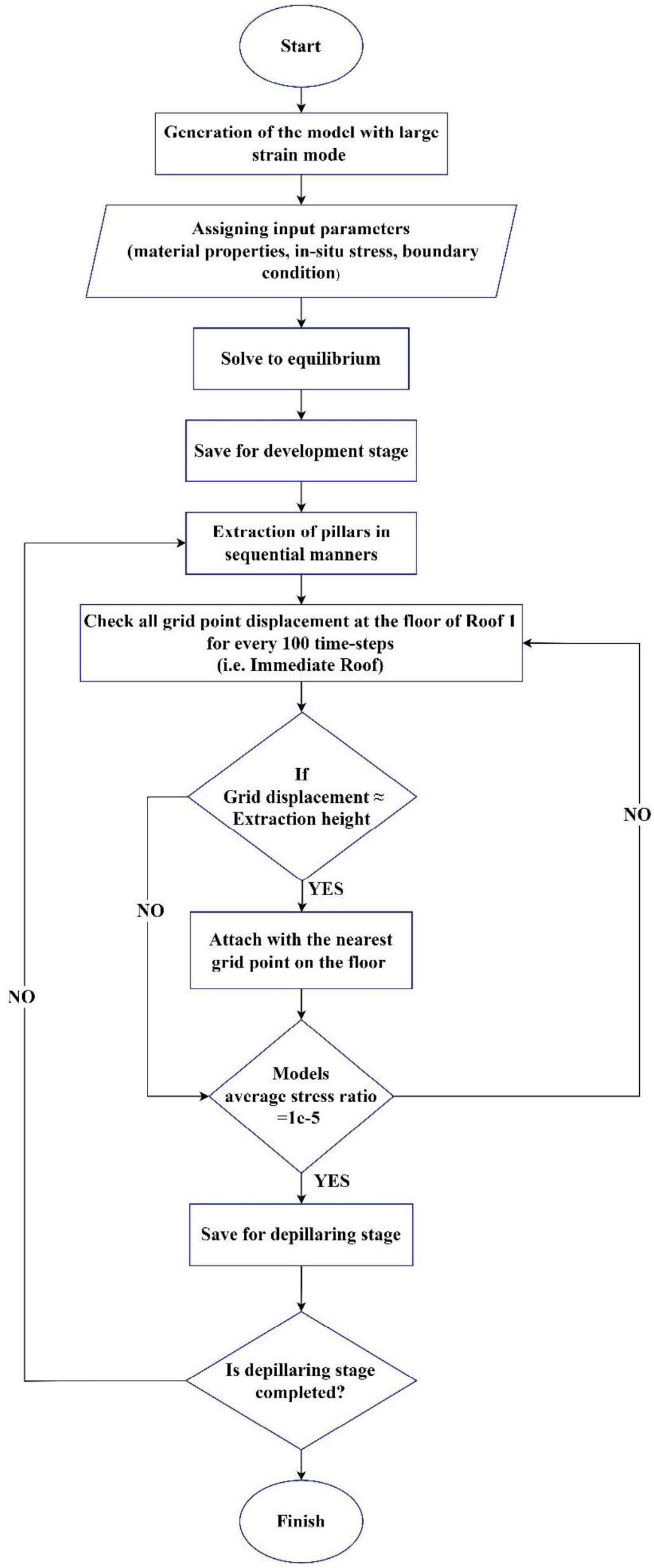

Figure 3.7: Flowchart of proposed numerical approach

3.4 Concluding remarks

A methodology for developing a time-dependent constitutive model and explicit caving simulation approach was discussed in this chapter. The time-dependent constitutive model employs an exponential relation of the post-failure Hoek-Brown strength parameters (m and s) concerning age and plastic strain. Implementation of the proposed time-dependent constitutive model in the FLAC^{3D} has been discussed. The proposed simplified caving simulation scheme during depillaring operations has also been highlighted.